

# ARTICLE IN PRESS

## Structural Modification, Strengthening Mechanism and Electrochemical Assessment of the Enhanced Conditioned AA6063-type Al-Mg-Si Alloy

O.S.I. Fayomi<sup>1,2,\*</sup>, O.P. Gbenedor<sup>2</sup>, M. Abdulwahab<sup>1</sup>, C.A. Bolu<sup>2</sup> and A.P.I. Popoola<sup>1,†</sup>

<sup>1</sup>Faculty of Engineering and the Built Environment, Tshwane University of Technology, P.M.B X680, Pretoria, South Africa

<sup>2</sup>College of Science and Technology, Covenant University, P.M.B 1023, Ota, Ogun state, Nigeria

Received: August 20, 2012, Accepted: September 12, 2012, Available online: September 25, 2012

**Abstract:** Enhancement of engineering materials is essential for averting service failure and corrosion attack in the industries. The impact of Ni as inoculant and solidification process on the corrosion resistance of an Al-Mg-Si alloy has been investigated in 3.65% NaCl solution using potentiodynamic polarization measurement. The alloying compositions and phase change were determined with energy dispersive spectroscopy (EDX) and x-ray diffraction (XRD). The surface morphology of the alloyed sample using scanning electron microscope (SEM) showed that Ni particles were well dispatched along the interface. The addition of Ni to Al-Mg-Si alloy led to the precipitation and crystallization of  $Al_2Ni$  and  $AlNi_2$  formed at the grain boundaries. Equally, as the percentage of Ni content increases in the alloy, the corrosion rate decreased due to the presence of  $Al_2Ni_3$  which proceeded at active regions. Inoculation of Ni particles coupled with increase in solidification reduces the possibility of corrosion penetration within the structural interface.

**Keywords:** Al-Mg-Si alloy, conditioning, electrochemical, surface morphology

### 1. INTRODUCTION

The demand and applications of aluminum and its alloy for different purposes especially in industrial and marine environment are mainly because of the excellent properties they possessed [1-20]. The reasons for its application can be traceable to its good mechanical, chemical and physical properties. More so, to obtain some special mechanical properties for aluminium product, metallic particulates are essential in a melt. This is as a result of the fact that, the soundness of every cast product can be achieved by grain refining, which entails increasing the rate of heat extraction, addition of grain refining agents and melt agitation [6-12]. For instance, some reports indicated that titanium or titanium-boride (Ti or TiB) particles inclusion in cast bath has been reported to enhance the metal stability and induced smaller grain size with low content [4,19]. Magnesium particle-inclusion in cast bath has been reported to induced crack and foster corrosion initiation instead of improving metal stability [20]. Nickel particle as a refiner for ferrous and nonferrous castings has been subject of interest over years. Some report have shown that this metal help to promote the formation of passive films resulting into a reduction in corrosion

rate [21,22]. Although grain refiners has been used to enhance aluminium alloy properties, but the study of the corrosion behavior is also very essential in evaluating the performance of the alloy behavior [23-25]. Mostly, aluminium has better corrosion resistance properties due to its thin film oxide formation. In acidic and chloride medium, the breakdown of the protective films occur [10-12,24-27]. In the present work, we considered it necessary to study the corrosion behavior of Al-Mg-Si-xNi alloy quenched in different cooling media.

### 2. EXPERIMENTAL

#### 2.1. Sample preparation

The alloys were prepared by liquid metallurgy method in a cast iron mould in the form of cylindrical castings (40 mm in diameter and 200 mm long) as reported elsewhere [23]. The Al in a graphite crucible was melted in an electric furnace under a nitrogen protective atmosphere. After melting of the Al to a temperature of 700 °C, elemental Ni particle was introduced to the melt and stirred thoroughly. This was allowed to stay for about 2-3 minutes during which the temperature was maintained for super heat to occur. The melts were then poured into permanent cast iron mould pre-heated to about 150 °C. The raw materials were pure Al (95 wt%) and Ni

To whom correspondence should be addressed:  
Email: \*sunnyfayomi@yahoo.co.uk, †popoolaapi@tut.ac.za

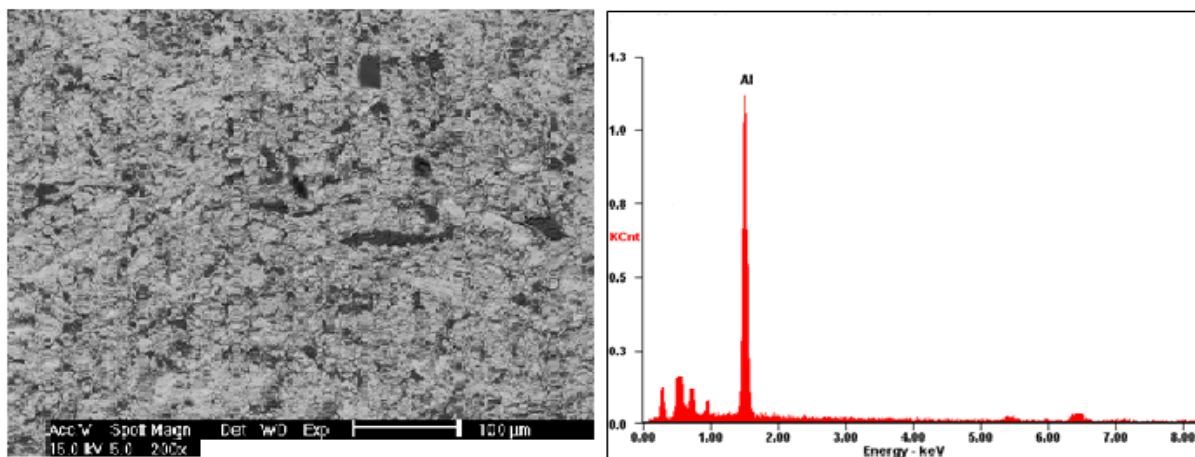


Figure 1. SEM micrograph and the EDS of AA6063 aluminium alloy used for the study

(99.95 wt%). Subsequently, five different Al-Ni based alloys having different cooling systems were prepared. Portions of the prepared sample were further taken for microstructural characterization, phase analysis and electrochemical study by using (SEM/EDS), XRD and linear potentiodynamic polarization method. The chemical compositions of the alloy were determined with spectrometer analyzer as shown in Table 1. The process of conditioning and solidification medium are indicated in Table 2.

## 2.2. Microstructure and surface characterization

After the casting process, the morphology of the alloyed samples and phase change were undertaken in terms of microstructure, composition and phases. Chemical reactions between molten aluminium and the metallic alloying agent led to the precipitation of different intermetallic compounds within the surface matrix. The following characterization tests were carried out: X-ray diffraction (XRD) analyses of quenched alloyed samples using a Philips PW 1713 X-ray diffractometer fitted with a monochromatic Cu K $\alpha$  radiation set at 40 kV and 20 mA was used to determine the phase composition. Phase identification was done using Philips Analytical X'PertHighScore® software with an in-built International Centre for Diffraction Data (ICSD) database. The surfaces of some

samples were analyzed using a scanning electron microscope (SEM) Model (Joel JSM-7500F).

## 2.3. Electrochemical examination

The electrochemical potentiodynamic technique was used to characterize the corrosion rate (Current densities) consisting of cyclic polarization. A potentiostat coupled to a computer system, a glass corrosion cell kit with a platinum counter electrode and a saturated Ag/Ag reference electrode were used. The working electrodes consist of the alloyed and the as-cast samples. The samples were positioned at the glass corrosion cell kit, leaving a 1 cm<sup>2</sup> alloy surfaces in contact with the solution. Polarization test were carried out in a 3.65wt% NaCl solution (3.65 g in 100mL of distilled water) at room temperature (RT) in a static solution for a period of 30 minutes each using a potentiostat. The polarization curves were determined by stepping the potential at a scan rate of 0.003V/sec. The polarization curves were plotted using Autolab data acquisition system (Autolab model: AuT71791 and PGSTAT 30) with (GPES) package version 4.9. The corrosion rate and potential were estimated by the Tafel extrapolation method (corrosion rate analysis) using both the anodic and cathodic branches of the polarization curves.

## 3. RESULTS AND DISCUSSION

### 3.1. Characterization of the as-cast and inoculated AA6063 aluminium alloy

Figure 1 shows the SEM micrograph and EDS spectra of pure Al-Mg-Si alloy indicating higher value of element Al. Al has the highest count with other metal un-identified within the energy level.

Effects of inoculant and cooling medium on microstructural changes for the as-cast and alloyed samples have been presented in Figure 2-5 with their microstructures. The effect of water as coolant (Figure 2a) shows a fine  $\alpha$  – Al solid precipitate at the surface. The solute atoms that formed clusters in the aluminium matrix were found to be distributed across the entire surface. More so, it was carefully noted that dendritic structure was broken down indicating the presence of a quasi-binary eutectic mixture of Ni and Al<sub>2</sub>Ni<sub>3</sub>.

Table 1. Spectro-chemical analysis of the produced Al-Mg-Si Alloy

Element	Al	Si	Mg	Fe	Cu	Mn	Ti	Cr
Composition (wt%)	95	0.45	0.50	0.22	0.03	0.03	0.02	0.03

Table 2. Processing method and designation of samples

Mass of Ni powder (wt%)	Solidification medium	Sample designation
-	Water	A
4.2	Water	B
4.2	Air	C
16.5	Water	D
16.5	Air	E

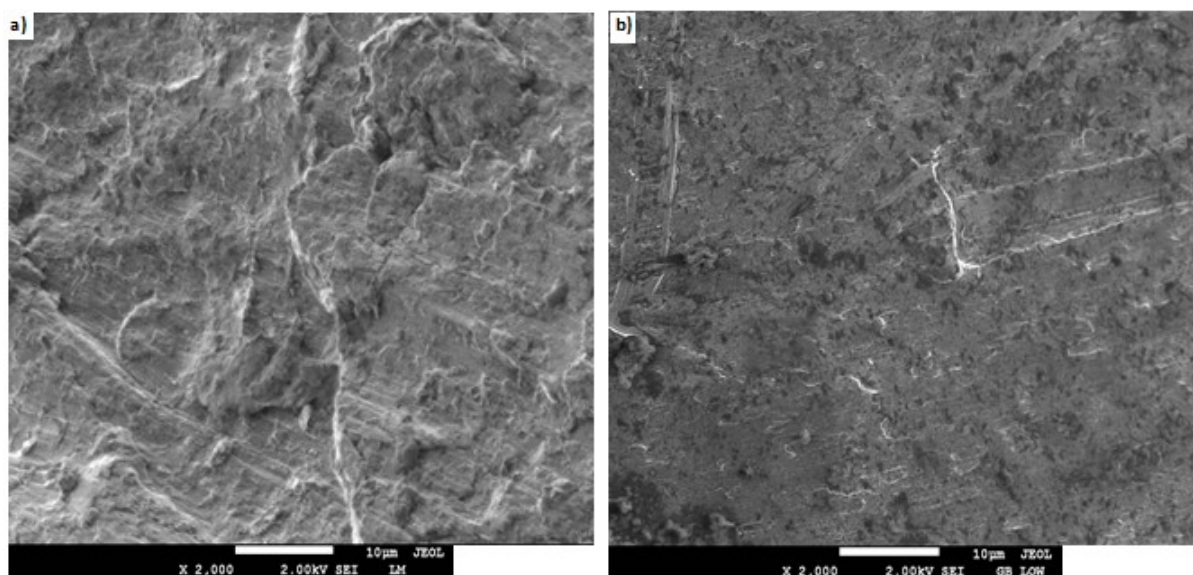


Figure 2. SEM micrographs of 4.2% Ni inoculated Al-Mg-Si alloy (a) water quenched (b) air cooled

along the grain boundaries region.

The surface morphology of the working alloyed sample In Figure 2a change due to 4.2% nickel in the Al melts. There by revealing the dendritic structure of a nickel alloy. It is reported that the microstructure of castings is of great importance due to its role in mechanical properties [8, 23,24]. The dendritic networks are enclosed by the eutectoid and eutectic phase precipitant indicating small particle of Ni, even though not evenly dispersed within the as-cast matrix was observed with higher magnification. Thus addition of 4.2% nickel to the Al-Mg-Si alloy and subsequent water cooling revealed a complex nickel-based intermetallic compound within the aluminium solid solution. This is in agreement with fact that structural refinement takes place due to the reduction of grain size owing to high solidification rate [9, 10].

The cooling medium has a noticeable influence on the surface morphological of the as-cast with dark crystals around the surface unlike the water quench medium which possesses fine grain size, good surface morphologies and interlock. This might be attributed to the grain refinement during solidification which restricted the alloy from fracture; thereby increasing the strength comparatively. Hence, the serviceability of components alloyed is determined to a large extent by the inoculant addition and the solidification processes employed. Moreso, it has been reported that addition of refiners to a melt resulted in microstructural changes leading to formation of complex intermetallic compounds [9, 23]. Equally, Figure 3 shows similar trend with the alloy containing 16.5% nickel addition which was air cooled. Except that nickel particles were also present at larger quantity with partial homogenization and formation a suitable phase of  $\text{Al}_2\text{Ni}$  and  $\text{Al}_3\text{Ni}_2$  clusters along the cast surface. Micro-segregation resulting from the water cooling of aluminium alloy causes limited eutectic transformation to occur, thereby forming eutectic within the region [15,19]. It was noted that the first phase to solidify was the aluminium rich phase appearing as primary dendrites which was attributed to the melting temperature of Al. This is followed by the eutectoid and of eutectic transformation

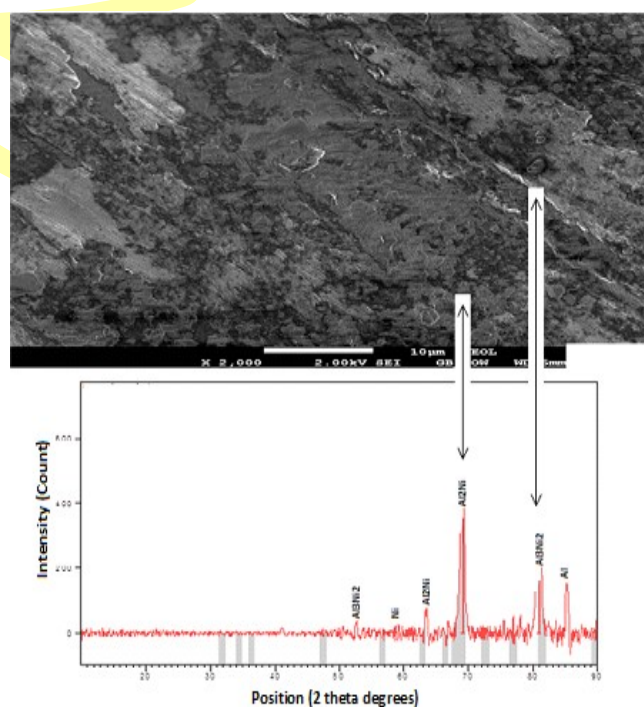


Figure 3. SEM micrograph and XRD spectrum of Al-Mg-Si-16.5% Ni alloy (water coolant).

leading to the occurrence of the phases in the inter-dendritic regions.

In Figure 4, the influence of air cooling was observed on the surface morphology of the as-cast sample. It can be seen that addition of 4.5 %wt of Ni to the alloy system altered the microstructures and resulted into formation of complex intermetallic compounds. The nucleation of nickel containing phase(s) could be at-



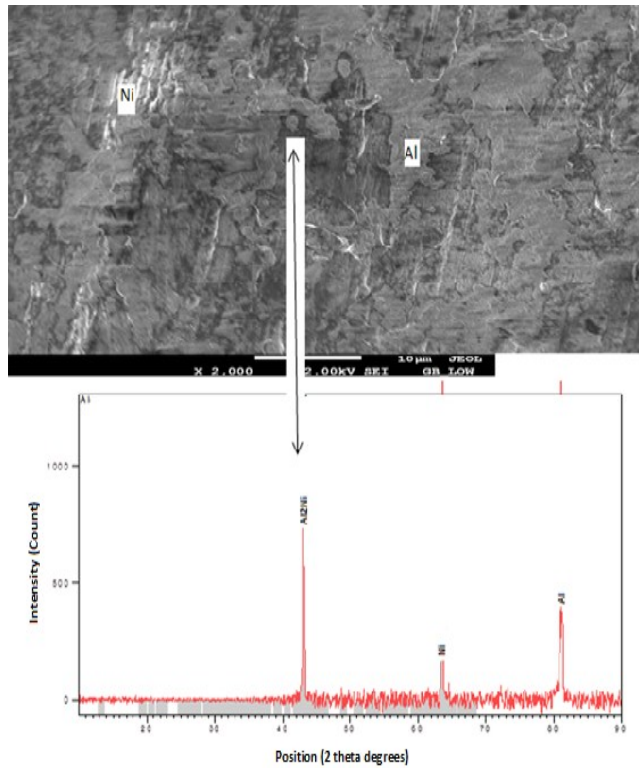


Figure 4. SEM micrograph and XRD spectrum of Al-Mg-Si-16.5% Ni alloy (air coolant).

tributed to the favourable sites for the nucleation offered by the aluminum particles that are formed first during solidification. Solidification process may also have contributed to the redistribution of the solute elements and the breakdown of the dendrites. These factors caused the alloy(s) to homogenize. The structure of the re-solidified regions, where partial melting had taken place (Figure 4) was due to a significantly higher rate of solidification experienced by the regions during quenching from high casting temperature [23]. It should be noted that the solid regions surrounding the molten ones act as a heat sink during the process of cooling thereby facilitating a higher rate of solidification and formation of stable phase.

More so, the electrochemical corrosion data (Table 3) and the polarization curves obtained as a result of Ni addition to Al-Mg-Si alloy are shown on Figure 5. As cast Al-Mg-Si alloy was used as a basis for comparison with the other alloy enhanced with different

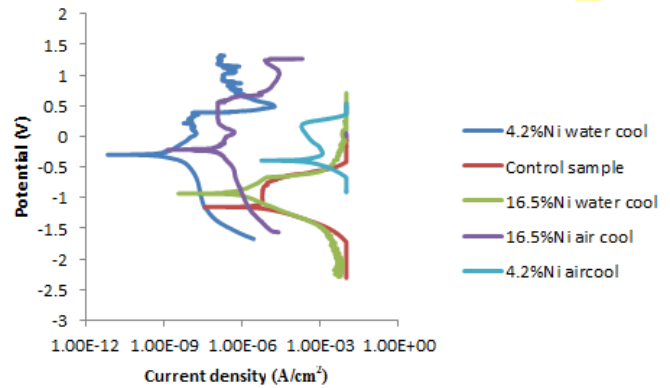


Figure 5. Cyclic polarization curves for as-cast Al-Mg-Si alloy and Ni alloyed Al-Mg-Si alloy in 3.65% NaCl solution at room temperature.

Ni percentage addition and solidification processes. It can be observed that all samples showed an active-passive behavior, with decreasing current densities and progressive increase in the corrosion potentials. On the linear scan, the corrosion potential of the inoculated sample; 4.2%wt Ni (water cool) was -0.3183 V, 4.2%wt Ni (air cool) is -0.4173, 16.5%wt Ni (water cool) is -0.9370 and 16.5%wt Ni (water cool) is -0.2195 while that of as-cast Al is -1.1694 V. These indicate that, the corrosion rate experienced with the inoculated sample is much lower, hence higher resistance observed in the curve. In order words, all alloyed samples proved that their corrosion is at the passive region than the pure Al sample (see Figure 5).

Comparatively, the alloyed Al-Mg-Si samples quenched in different media have higher polarization resistance value ( $R_p$ ) than as-cast sample (Table 3 and Figure 5) and hence, the lowest corrosion rate, was achieved with the alloyed Al-Mg-Si samples.

The lowest corrosion rate and the highest  $R_p$  value was for the solidified and enhanced 4.2%wt Ni (water cool), indicating a more stabilized and protective alloy than the other and far above the unalloyed sample with polarization resistance difference of  $2.47 \times 10^6$  as compare to the unalloyed sample. This occurrence can be attributed to the precipitation of  $Al_2Ni$  and  $Al_3Ni_2$  within the alloyed matrix. Therefore an increase in  $R_p$  was achieved as a result of enhanced Ni inoculation and solidification.

More so, the existence of anodic inter-phase, such as  $Al_2Ni_2$   $Al_3Ni_2$  particles in Figure 3 and 4, during the alloy formation and particle solidification accelerated the possibility of hydrolysis reaction. This has been reported elsewhere [11, 20], that once hydroly-

Table 3. Potentiodynamic polarization data obtained from Tafel plot for as-cast Al-Mg-Si and alloyed Al-Mg-Si samples

Sample type	$i_{corr}$ (A)	$I_{corr}$ (A/cm <sup>2</sup> )	LPR $R_p$ ( $\Omega$ cm <sup>2</sup> )	$-E_{corr}$ (V)	Corrosion rate (mm/yr)
As-received	3.77E-4	3.77E-4	1.24E+1	1.3514	$2.43 \times 10^{-1}$
A1, 4.2%wt Ni (water cool)	1.71E-9	1.71E-9	3.61E+7	0.3183	$2.67 \times 10^{-5}$
A2, 4.2%wt Ni (air cool)	3.95E-7	3.95E-7	2.55E+2	0.4173	$6.15 \times 10^{-3}$
A3, 16.5%wt Ni (water cool)	2.42E-7	2.42E-7	5.58E+2	0.9370	$3.68 \times 10^{-3}$
A4, 16.5%wt Ni (air cool)	3.79E-8	3.79E-8	6.60E+3	0.2195	$5.77 \times 10^{-4}$

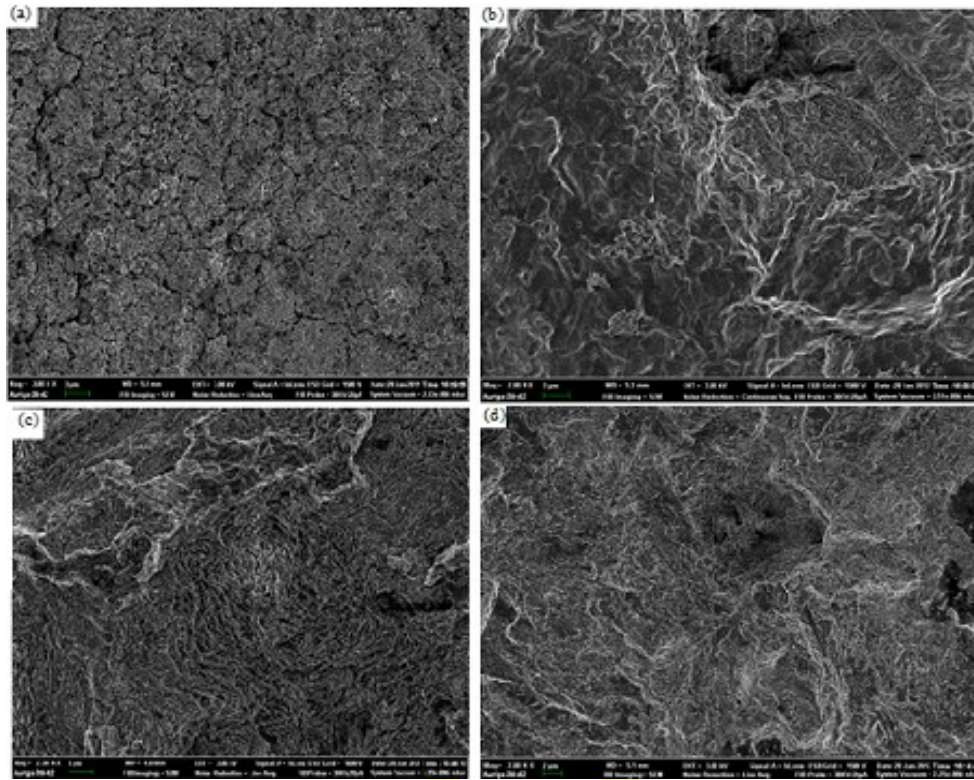


Figure 6. SEM micrographs of the as-corroded surfaces of the Al-Mg-Si alloys containing a) 4.2% Ni (water coolant) b) 4.2% Ni (air coolant) c) 16.5% Ni (water coolant) d) 16.5% Ni (air coolant) in 3.65% NaCl solution.

sis reaction starts, corrosion reaction can proceed by oxidation. Consequently,  $Cl^-$  adsorbed on the oxide film sites causing the breakdown of the layers by the initial-existing protective oxide film. The chloride ion then reacts with the aluminium hydroxide which results into pitting corrosion. The formation of  $Al^{3+}$  was as a result of an increase in the anodic current.

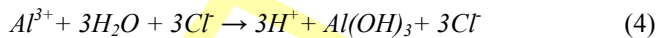
Possible metallurgical reaction shown below could occur as a result of the hydrolysis process.



Oxygen reduction at the cathodic reaction:



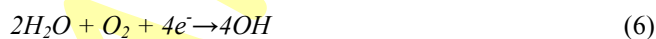
Hence, equation 1 and 2 lead to equation 3 with formation of metal hydroxides:



Hence, alloy formation conditioned with inoculant may proceed with oxidation process



The  $Ni^{2+}$  and  $Al^{3+}$  ions formed after oxidation of Ni ( $Al \rightarrow Al^{3+}$ ,  $Ni \rightarrow Ni^{2+}$ ), while  $OH^-$  releases after oxygen reduction:



Because of solubility of  $Ni(OH)_2$  and  $Al(OH)_3$  in the solution there is a tendency of corrosion products formed at the metal/solution interfaces of the Al-Mg-Si-Ni alloy. Formation of this existing particulate may however be the main reason for the occurrence of the diffusion behaviour in the interface of the alloy.

Figure 6 shows the SEM micrographs of Al-Mg-Si alloyed with different weight percentage of Ni and cooling medium after exposure in 3.65 % NaCl solution using polarization method. Few pits were observed on the surface of the alloy due to the heterogeneous occurrences between the enhance particle on the Al. Though, from their XRD earlier shown, it was evident in alloyed surface an inter-metallic phases of  $NiAl$ ,  $Ni_3Al$ ,  $NiAl_3$ , and  $Al_3Ni_2$  in the form of fine dendritic structures. On the other hand, the passive film can be said to have been disrupted by aggressive chloride ions, and initiate a localized corrosion (Fig. 6a). The surface degradation observed on the alloyed samples may be as a result of occurrence of interdendritic boundaries occurring between the two metals inoculated (the base metal and the inoculant). Previous report affirmed that the corrosion process also takes place at the metal-medium phase boundary [10]; therefore it is a heterogeneous reaction in which the structure and condition of the metal's surface have a significant role. These interdendritic boundaries have been reported to have higher tendency to corrosion attacks due to the presence of second phase particles [26,27].

The microstructure of the alloy containing 4.2% Ni air and water cooled (Fig. 6 a and b) reveals the presence of dendritic structure and inter-diffused boundary especially with Figure 6a while Fig. 6

c and d the formation of secondary phases between the dendrite sites is not observed clearly which is an indication of fine precipitate phase and proper conditioning of the particulate within the base alloy.

#### 4. CONCLUSIONS

1. Harnessing of Ni to the Al-base alloy led to the precipitation of  $\text{Al}_2\text{Ni}_3$  intermetallic compounds along grain boundaries.
2. The electrochemical parameters obtained from polarization curves showed that increase in Ni contents resulted to a decrease in the corrosion current density. The magnitude of the polarization resistance value,  $R_p$ , increases with an increase in the Ni contents.
3. It was also affirmed that with the presence of Ni contents, aluminum with refined structure can be obtained with the addition of 16.2 wt% of Ni powder coupled with water cooling.
4. That the corrosion process was controlled by the adsorption of the re-inforced ions from the particulate and the well dispatched dissolution of the precipitate.

#### 5. ACKNOWLEDGMENTS

This material is based upon work supported financially by the National Research Foundation. Covenant University, Ota, Ogun State, is appreciated for equipment support.

#### REFERENCES

- [1] L.A. Dobrzański, R. Maniara, J.H. Sokolowski, J. Achiev. Mater. Manuf. Eng., 17, 217 (2006).
- [2] H. Nguyen, School of Engineering, Grand Valley State, 1, (2005).
- [3] F. Grosselle, G. Timelli, F. Bonollo, R. Molin, Metall. Sci. and Tech., 22, 2 (2009).
- [4] C.K. Sigworth, T.A. Khun, American Foundry Society, 1, 12 (2007).
- [5] J. Szajnar, T. Wróbel, J. Achiev. Mater. Manuf. Eng., 27, 95 (2008).
- [6] X. Bo, L. Yuandong, Y. Ma, H. Yuan, China Foundry, 8, 121 (2011).
- [7] R.Y. Chen, D.J. Willis, Metall. Mater. Trans., 36, 117 (2005).
- [8] S. Yanwei, L. Bangsheng, L. Aihui, G. Jingjie and F. Hengzhi, China Foundry, 7, 43 (2010).
- [9] T. Ahmet, D. Mehmet, K. Sabri, J. Mater. Sci., 42, 8298 (2007).
- [10] A.P.I. Popoola, S.L. Pityana, O.M. Popoola, Int. J. of Elec. Sci., 6, 5038 (2011).
- [11] A.P.I. Popoola, S.L. Pityana, O.M. Popoola, The J. of the South African Inst. of Min. and Met., 111, 345 (2011).
- [12] Y. Chuang, S. Lee, H. Lin, Mat. Trans., 47, 106 (2006).
- [13] M. Abdulwahab, I.A. Madugu, S.A. Yaro, S.B. Hassan, A.P.I. Popoola, Mat. Des., 32, 1159 (2011).
- [14] N. Li, X. Lu, C. Jian-Zhong, Trans. of Nonfer. Met. Soc. of China, 18, 541 (2008).
- [15] F. Bonollo, J. Urban, B. Bonatto and M. Botter, Aluminium Elegh; la metallurgia italiana, 6, 23 (2005).
- [16] H.S. Ding, J.J. Gou and J. Jia, Trans. Nonferrous Met. Soc. China, 11, 540 (2001).
- [17] J. Deshpande, Research Programs. Department of Manufacturing Engineering, Worcester Polytechnic Institute (2006).
- [18] D. Vander Boon, Laboratory module 3, Grand Valley State University 1, 5 (2005).
- [19] A. Rashid, BUET Dhaka lectures, 7, 1 (2010).
- [20] S. Vuelas, S. Valdez, J.G. Gonzalez-Rodriguez, Int. J. Electrochem. Sci., 7, 4171 (2012).
- [21] T. Aburada, M. James, F. Gerald, J.R. Scully, ECS Trans, 16, 19 (2009).
- [22] K. Hashimoto, M. Naka, T. Masumoto, The 1660<sup>th</sup> report of the research institute of iron and steel, 48, (1979).
- [23] O.P. Gbenedor M. Abdulwahab, O.S.I. Fayomi, A.P.I. Popoola, Chalcogenide Letters, 9, 201 (2012).
- [24] A.P.I. Popoola, O.S.I. Fayomi, M. Abdulwahab, Int. J. Electrochem. Sci., 7, 5827 (2012).
- [25] A.P.I. Popoola, O.S. Fayomi, Int. J. Electrochem. Sci., 6, 3254 (2011).
- [26] A.P.I. Popoola, O.S.I. Fayomi, O.M. Popoola, Int. J. Electrochem. Sci., 7, 4898 (2012).
- [27] O.S.I. Fayomi, A.P.I. Popoola, Int. J. Electrochem. Sci., 7, 6555 (2012).